

# Beyond $zT$ : Is There a Limit to Thermoelectric Figure of Merit?

YURIY LOBUNETS <sup>1,2</sup>

1.—Solid Cell Inc., 771 Elmgrove Rd., Rochester, NY 14624, USA. 2.—e-mail: yuriy.lobunets@solidcell.com

The concept of the dimensionless thermoelectric figure of merit  $zT$  was derived by A.F. Ioffe and has been widely used to assess the desirability of thermoelectric materials for devices. Solid state physics does not set limits on this criterion, but it can be shown that such restrictions are imposed by the laws of thermodynamics. The physical meaning of  $zT$  can be interpreted as the ratio of the virtual efficiency of a thermoelectric generator (TEG)  $\eta_o$  and the Carnot efficiency  $\eta_c$ :  $zT = \eta_o/\eta_c$ . Hence, the conclusion about the  $zT$  restriction:  $\lim(zT) \leq 1$ , which is correlated with the data on the properties of well-studied thermoelectric materials, but contradicts much new experimental data. This contradiction serves as a pretext for further study of possible constraints on  $zT$ . An additional bonus from this analysis is the possibility of the experimental determination of  $zT$  by direct measurement of temperatures, heat flux, and open circle voltage. An analysis of the expanded mathematical model of a TEG shows that the influence of the Biot criterion on the power capacity of the TEG significantly exceeds the influence of  $zT$ . That is, it is possible to compensate for the high thermal conductivity of materials due to more intense heat transfer. This approach to improving the characteristics is demonstrated by developing a TEG for the conversion of latent heat of liquid natural gas (LNG).

**Key words:** Thermoelectric figure of merit, specific power of thermoelectric generator, CryoTEG

## List of Symbols

Bi	Biot criterion	$t_h$	Heat carrier temperature (K)
$I$	Electrical current (A)	$t_c$	Coolant temperature (K)
$j$	Current density (A/cm <sup>2</sup> )	$\Delta t$	Temperature difference heat carriers (K)
$J$	Dimensionless current density	$\Theta = T/T_o$	Dimensionless temperature
$e$	Seebeck coefficient (V/K)	$\theta = t/T_o$	Dimensionless temperature of fluid
$E$	Electromotive force (V)	$z$	Thermoelectric figure-of-merit (K <sup>-1</sup> )
$\lambda$	Thermal conductivity (W/cm-K)	$zT_o$	Dimensionless thermoelectric figure-of-merit
$\sigma$	Electrical conductivity (Ω/cm)	$N$	Electrical power (W)
$h$	Thermocouple leg length (cm)	$N_x$	Dimensionless power
$n$	Number of thermoelectric elements on module	$Q$	Heat power flow (W)
$s$	Thermoelectric leg cross sectional area (cm <sup>2</sup> )	$\eta$	Efficiency
$T_o$	Determining temperature (K)	$\eta_c$	Carnot efficiency
$T_h$	Hot junction temperature (K)	$\alpha$	Heat transfer coefficient (W/cm <sup>2</sup> K)
$T_c$	Cold junction temperature (K)	$R_{\alpha,\lambda}$	Thermal resistance (cm <sup>2</sup> K/W)
$\Delta T$	Junction temperature difference (K)	$R$	Electrical resistance (Ω)
		$R_L$	Electrical load resistance (Ω)
		$m = R_L/R$	Load factor
		LCOE	Levelized cost of electricity (\$/kWh)
		$Y = y/h$	Dimensionless coordinate

(Received August 21, 2018; accepted January 8, 2019; published online January 18, 2019)

**INTRODUCTION**

The modern paradigm of the development of thermoelectric devices is based on an increase in the thermoelectric figure of merit of thermoelectric materials  $zT$ , which determines the theoretical efficiency limit of thermoelectric generators and heat pumps. A concept thermoelectric figure of merit  $zT$  was derived by Ioffe<sup>1</sup> considering the problem at a fixed temperature of the hot and cold thermocouple junction  $T_h$  and  $T_c$ . In terms of obtaining maximum efficiency of energy conversion  $\eta_{max}$ , this criterion together with the Carnot efficiency  $\eta_c$  is crucial:

$$\eta_{max} = \eta_c \frac{\sqrt{1 + zT} - 1}{\sqrt{1 + zT} + 1 - \eta_c} \quad (1)$$

In (1)  $T$  is the average value of the known temperatures  $T = (T_h + T_c)/2$ , which leads to some uncertainty. Clearly, the case  $T = const$  is an abstraction that cannot be put into practice because the junction temperature is a function of the state of the system and depends on many parameters. For the real devices the mathematical model is more correct in the boundary conditions of the third kind—that is, under the given conditions of heat exchange.

**MATHEMATICAL FORMULATION**

In fact, the temperatures of the junction  $T_h$  and  $T_c$  depend on the conditions of heat transfer in the system “Heat Source–Thermocouple–Heat Sink”. The most appropriate mathematical model to describe the thermoelement (TE) is thus a nonlinear with boundary conditions of the third kind (convection boundary conditions), as it considers the mechanism of heat transfer and balances the heat on the TE surfaces.<sup>2</sup> The calculation scheme is shown in Fig. 1.

The mathematical model of the thermoelement consists of:

- one-dimensional equation of thermal conductivity of a thermoelement:

$$\frac{d^2T}{dy^2} + \frac{j^2}{\lambda\sigma} = 0; \quad (2)$$

- the equation of thermal balance on a hot surface ( $y = h$ ), which consists of the thermal flow of heat conduction  $Q_\lambda = -\lambda \frac{dT}{dy}$ , the heat flux of heat exchange  $Q_{zh} = \alpha_h(t_h - T(h))$ , and heat of Peltier  $Q_\pi = jeT(h)$ :

$$\lambda \frac{dT}{dy} - jeT(h) + \alpha_h(t_h - T(h)) = 0; \quad (3)$$

- a similar equation of thermal balance on a cold surface ( $y = 0$ ):

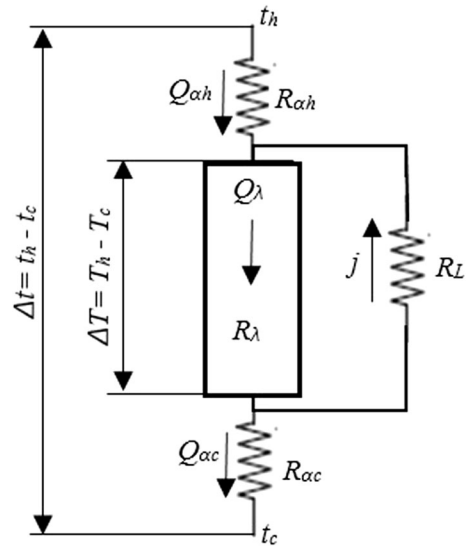


Fig. 1. Scheme for calculating the thermoelement.

$$\lambda \frac{dT}{dy} - jeT(0) + \alpha_c(T(0) - t_c) = 0; \quad (4)$$

- and the equation for current density in a circle:

$$j = e(T(h) - T(0))/(h/\sigma + R_L). \quad (5)$$

The available temperature difference  $\Delta t = (t_h - t_c)$  is divided between the TE and the heat exchangers (heat source/heat sink) proportionately to the values of their thermal resistances  $R_\lambda, R_{zh}, R_{zc}$ , which include thermal resistance of heat transfer and thermal resistances  $R_i, R_k$  of all intermediate layers on each side:

$$R_\lambda = \frac{h}{\lambda}; \quad R_{zh} = \frac{1}{\alpha_h} + \sum_1^i \frac{h_i}{\lambda_i}; \quad R_{zc} = \frac{1}{\alpha_c} + \sum_1^k \frac{h_k}{\lambda_k} \quad (6)$$

The mathematical model (2–5) may be simplified by considering it in dimensionless form. Reference 2 demonstrated that the problem of thermoelectric energy conversion can be reduced to a small-size system of generalized variables having clear physical meaning and normalized variation intervals:

$$N_x = f(zT_o, Bi, J). \quad (7)$$

where  $N_x = Nh/\lambda T_o$ , the dimensionless power;  $zT_o$ , the dimensionless thermoelectric figure of merit ( $z = e^2\sigma/\lambda$ );  $Bi = \alpha h/\lambda$ , the Biot criterion;  $J = jeh/\lambda$ , the dimensionless current.

Consequently, the mathematical model of problems (2–5) may be written as:

Dimensionless thermal conductivity equation:

$$\frac{\partial^2 \Theta}{\partial Y^2} + \frac{J^2}{zT_o} = 0; \tag{8}$$

Dimensionless equation of thermal balance on a hot surface:

$$Bi_h[\theta_h - \Theta(1)] + \Theta'(1) - J\Theta(1) = 0; \tag{9}$$

Dimensionless equation of thermal balance on a cold surface:

$$Bi_c[\Theta(0) - \theta_c] + \Theta(0) - J\Theta(0) = 0; \tag{10}$$

The solutions of Eq. 8 have the form:

$$\Theta(Y) = C_1 + C_2 Y - \frac{J^2}{2zT_o} Y^2, \tag{11}$$

Substituting (11) into (9, 10), we get the following system of equations for the determination of constants  $C_1, C_2$ :

$$C_1(J + Bi_h) - C_2 = Bi_h\theta_h; \tag{12}$$

$$C_1(Bi_c - J) + C_2(Bi_c - J + 1) = Bi_c\theta_c + \frac{J^2}{zT_o} \left(1 + \frac{Bi_c - J}{2}\right); \tag{13}$$

Solving the model (11–13) allows you to calculate the temperature mode and define all the parameters of the TEG. This enables us to find the *Pareto set*, which gives all possible solutions to the problem of thermoelectric energy conversion in the domain of defined variables, (Fig. 2). Analysis of such sets gives an idea of the basic properties of the system, the nature of the interaction of aggregates with each other, allows us to select in this space a set of effective solutions. The solutions to the problem obtained by generalized variables are universal, since cover all possible combinations of primary independent variables, and allow in the early stages of design to assess the possible characteristics of TEG.

## RESULTS AND DISCUSSION

### $zT$ Limitation

Figure 3 shows the dependencies of real temperature differences of junction  $\Delta T$  of the thermoelectric module on the load mode. The temperature difference in thermocouples in short circuit mode ( $m = 0$ ) reaches a minimum and gradually increases with load. In this case, the growing of  $\Delta T$  reaches 30 K. It accordingly affects the TEG capacity and efficiency. Figure 4 shows the dependence of the total ( $N_S$ ) and useful ( $N_L$ ) capacity in load mode. The total capacity of a TEG is the electric power that is supplied to the electrical circuit. The electrical resistance of the circuit is equal to the sum of the internal resistance  $R$  of

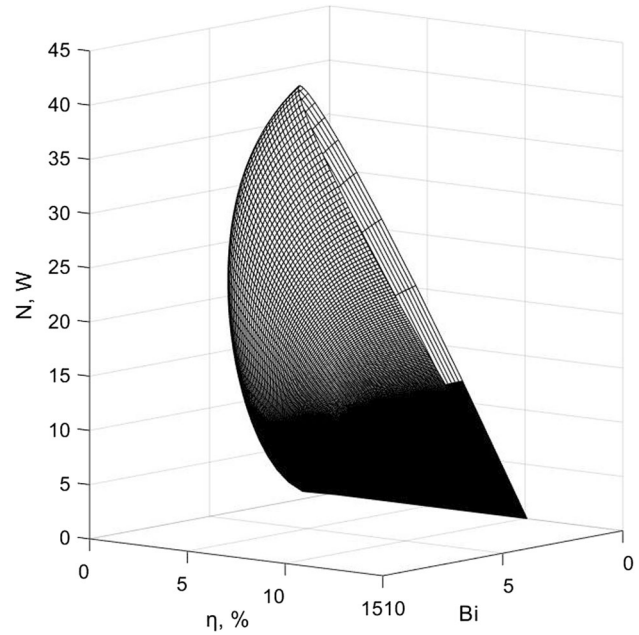


Fig. 2. Pareto set of the  $N$ - $\eta$ - $Bi$  for TEG.

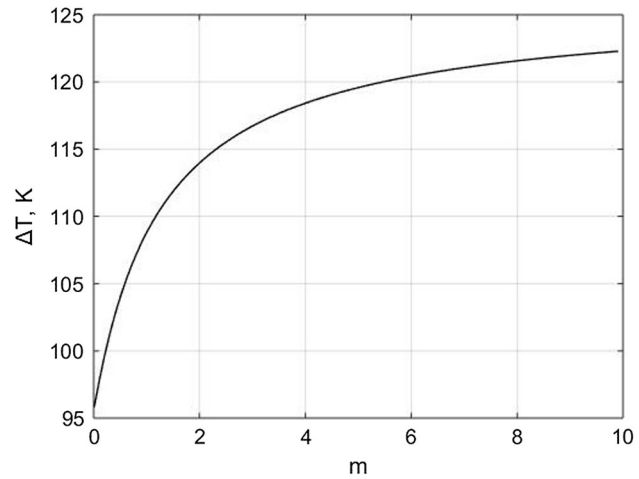


Fig. 3. Temperature drop  $\Delta T = T_h - T_c$  versus  $m = R_L/R$ .

thermocouples and payload  $R_L$ . Useful power  $N_L$  is a power that falls on the payload  $R_L$ . The total capacity of a TEG  $N_S$  reaches a maximum in short circuit mode ( $m = 0$ ) and is  $N_{marg} = (e\Delta T)2/R$ . To a clear physical meaning of the criterion  $zT$ , defining temperature  $T$  should be equal to maximum permissible working temperature  $T_o = t_h$ . Such a scale selection limits the range of possible dimensionless temperatures to the values  $\Theta = T/t_h \leq 1$ , which corresponds to the requirements of the theory of similarity. By simple changes, the following expression is obtained:

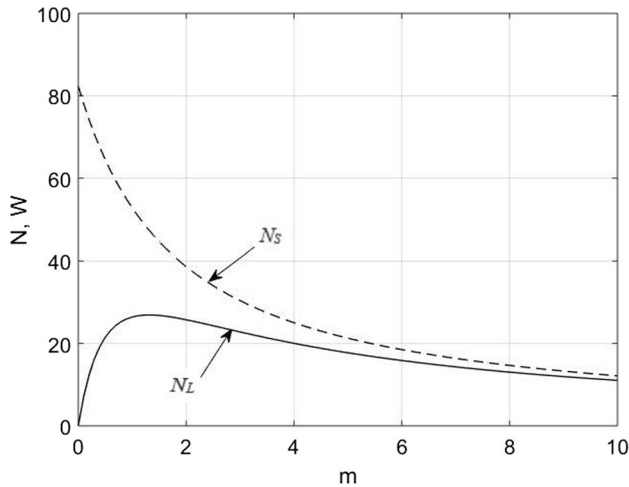


Fig. 4. Power  $N$  versus  $m = R_L/R$ .

$$N_{\text{marg}} = \frac{(e\Delta T)^2}{R} = \frac{e^2\sigma}{\lambda} T_o \frac{\Delta T}{T_o} \lambda \frac{\Delta T}{h} \quad (14)$$

Defining that  $Q_\lambda = \lambda\Delta T/h$ ;  $\eta_o = N_{\text{marg}}/Q_\lambda$ ; and  $\eta_c = \Delta T/T_o$ , we obtain the expression:

$$zT_o = \eta_o/\eta_c \quad (15)$$

The power of  $N_{\text{marg}}$  is a maximum as possible in the conditions under consideration. The heat flux of heat conductivity  $Q_\lambda$ , in turn, is minimally possible. Accordingly, the ratio of these variables provides the maximum of the  $zT_o$  criterion. From Eq. 15 follows that the thermoelectric figure of merit  $zT_o$  is the ratio of the virtual marginal efficiency of TEG  $\eta_o$  to the Carnot efficiency  $\eta_c$ . From the last expression comes the conclusion, in contrast to contemporary ideas about the limits of the thermoelectric figure of merit—since efficiency  $\eta_c$ , according to Carnot’s theorem,<sup>3</sup> determines a limit for the efficiency of the heat energy converter into electric power, is a fair limitation:

$$\lim(zT_o) \leq 1 \quad (16)$$

This finding is correlated with data on well-studied thermoelectric materials, such as  $\text{Bi}_2\text{Te}_3$ ,  $\text{PbTe}$ , and  $\text{Zn}_4\text{Sb}_3$ . However, there is enough new experimental data shows  $zT_o > 1$ ,<sup>4</sup> but the explanation of this discrepancy does not exist. Perhaps this is because the used mathematical model does not take into account the dependence of the properties of the material on temperature. So far, this issue has not been discussed in the literature, and its resolution requires a separate study. In any case, such a study may clarify the issue of the existence of the thermodynamic restrictions on  $zT$ .

Based on (14) proposed an indirect method of measuring the thermoelectric figure of merit  $zT_o$ .<sup>5</sup>

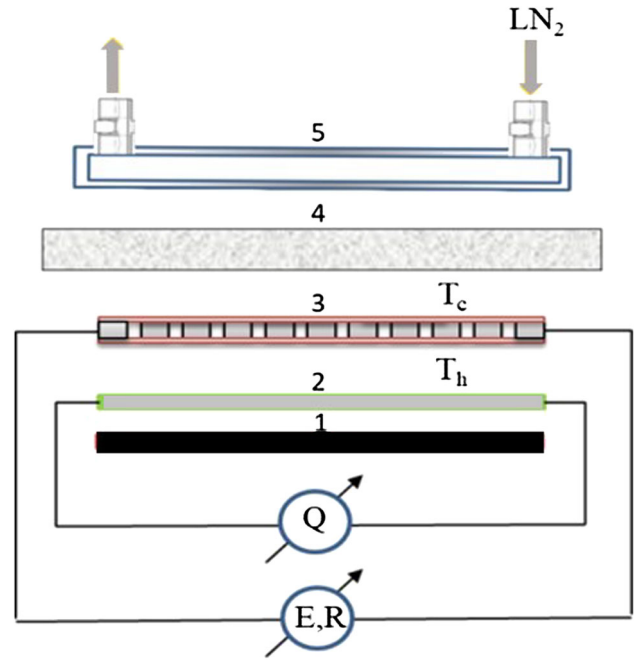


Fig. 5. Setup for measuring  $zT_o$ .

For the thermoelectric module  $zT_o$  can be represented as the ratio:

$$zT_o = \frac{E^2}{R} \cdot \frac{1}{Q} \cdot \frac{1}{\eta_c}, \quad (17)$$

where  $E = en\Delta T$ —electromotive force (EMF) of the thermoelectric module in idle mode;

$R = \frac{hn}{\sigma_s}$ , electrical resistance of the module;  $Q = \frac{\lambda sn}{h} \Delta T$ , heat flow of thermal conductivity;  $\eta_c = \frac{\Delta T}{T_o}$ , Carnot efficiency.

All components of Eq. 17 can be directly measured. Unlike the well-known Harman method,<sup>6</sup> it is not necessary to pass a current through the sample and separately determine the Seebeck coefficient and electrical conductivity. This simplifies the hardware implementation of the method and makes it possible to increase the accuracy of the measurements. The most significant error is associated with the measurement of heat fluxes ( $\leq 3\%$  using state-of-the-art heat flow sensor). This enables using the method for express control of the properties of thermoelectric modules under different temperature conditions. A diagram of the setup for measuring the thermoelectric figure of merit of the modules is shown in Fig. 5. With the help of the electric heater (1), the heat flux  $Q$  is set, which is controlled by the heat flux sensor (2). Passing through the thermoelectric module (3), the heat flux creates a temperature difference  $\Delta T = T_h - T_c$ , as a result the module generates an EMF  $E = en\Delta T$ . The module is cooled by a heat exchanger (5). Using the heater (1) and additional thermal resistance (4), the required temperature regime of the sample is

set. The unit is equipped with a set of instruments that measure and record all parameters necessary to determine the thermoelectric figure of merit  $zT_o$  according to expression (17).

**Performance Criteria of TEG**

Since the thermal conductivity  $\lambda$  is a component of both the defining criteria ( $zT$  and  $Bi$ ), consider its impact on the efficiency of a TEG. For the model, we assume that it is possible to reduce the coefficient of heat conductivity without changing other characteristics of the material. In our model, we employ the following  $\lambda = 0.005:0.02$  W/cmK. Accordingly, the figure of merit varies in the range of  $zT_o = 0.6:2.38$ , and  $Bi = 0.1:25$ . As Figs. 6 and 7 illustrate, the set of curves  $N = f(Bi)$  and  $\eta = f(Bi)$  is limited from below by the curve corresponding to  $zT_o = 0.6$ , and from above— $zT_o = 2.38$ .

The difference between the levels of curves illustrates the sensitivity of the TEG power and efficiency to parameter  $zT_o$ . This indicates that in real condition even a significant increase in the thermoelectric figure of merit at the expense of the thermal conductivity coefficient  $\lambda$  of the material is not critical for improving the power capacity of the TEG. Moreover, the desired effect can be achieved simply by the intensification of heat transfer. In addition, in expression  $Bi = \alpha h / \lambda$ , parameters  $\alpha$  and  $h/\lambda$  have the same weight, meaning that by the provision of high enough  $\alpha$ , a significant reduction  $h$  can be achieved. That would allow for both increasing of a TEG's capacity and of cost reduction of thermoelectric material used. For example, for  $\alpha = 1$  W/cm<sup>2</sup> K, the possible reduction of leg length  $h$  from the level cited in Refs. 7–9 ( $\alpha = 0.01$  W/cm<sup>2</sup> K,  $h = 4$  mm) to the much more economical  $h = 0.2$  mm. This reduces the cost of thermoelectric materials per unit of capacity 400 times.

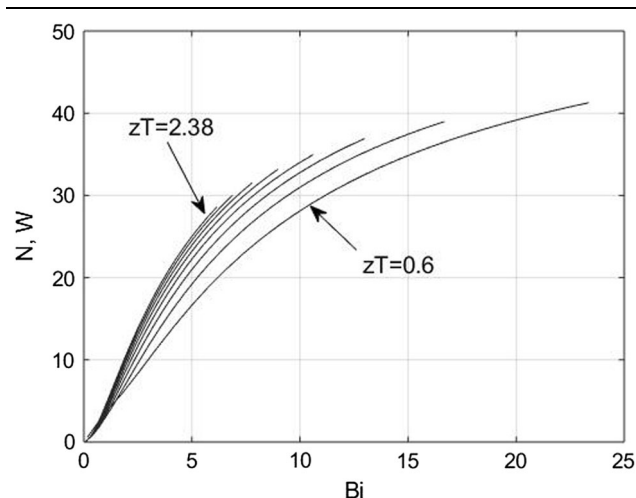


Fig. 6. Power of a TEG  $N$  versus  $Bi$ .

Such a conceptual approach is employed in the development of a TEG integrated into the LNG evaporator to make use of latent heat of the cryogenic liquid. Today, approximately 200 billion kWh of heat energy is wasted annually at regasification LNG terminals around the world, representing a huge addressable market for the proposed technology.<sup>10,11</sup> The effectiveness of TEGs in cold energy recovery based on existing technology has been demonstrated at the laboratory scale to have comparable or better performance than conventional Rankine cycle technology. A laboratory prototype of a cryogenic TEG has provided data supporting an indicative electricity generation cost of LCOE  $\approx$  \$0.015/kWh. Figure 8 shows the calculated dependence of the TEG power  $N$  on the square matrix of heat transfer coefficients  $[\alpha_h, \alpha_c] = [0.01:0.5]$ . Contour lines determine the power of

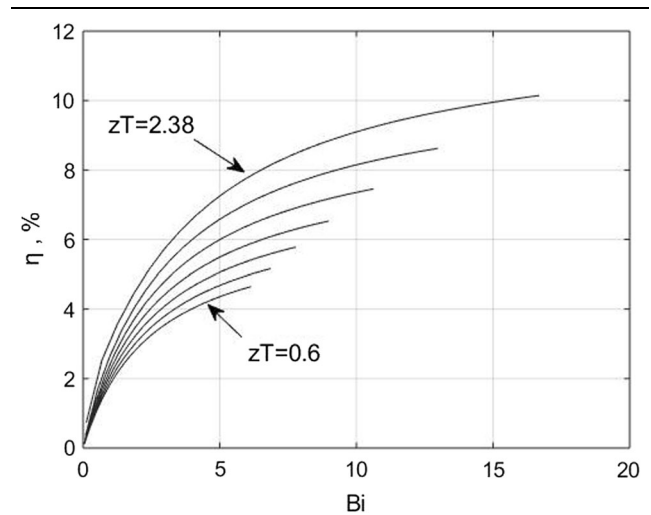


Fig. 7. Efficiency of a TEG  $\eta$  versus  $Bi$ .

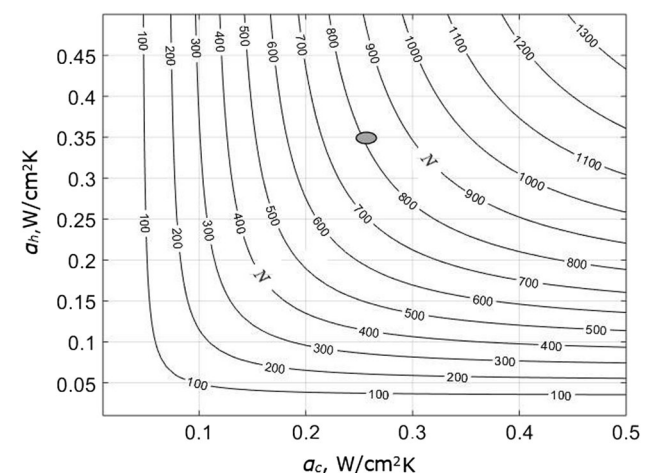


Fig. 8. TEG Power dependence from heat exchange intensities  $\alpha_c$  and  $\alpha_h$ .



the TEG  $N$ ,  $W$ , and the zone, limited by the grayed out oval, is experimental data. Measures to intensify heat exchange allowed the use of thermoelectric modules with a small leg length (0.8 mm), which ensured an increase five- to eightfold the specific power of designed TEG compared to state-of-the-art TEG.<sup>12</sup>

### CONCLUSION

The modern approach toward development of thermoelectric devices focuses primarily on increasing the thermoelectric figure of merit of the thermoelectric materials  $zT_o$ . The value of this criterion is limited by the laws of thermodynamics. In the low-temperature range materials have reached this limit. On the other hand, there is enormous untapped potential for performance improvements with these known materials, associated with loss of temperature difference during heat exchange. Optimization of the conditions of heat transfer within the system Heat Source–TEG–Heat Sink facilitates the use of this potential, which may significantly increase specific power and lower the cost of TEGs. This concept was the basis for the designed demonstration prototype of a TEG. As a result, the specific power of the prototype increased five to eightfold fold, and LCOE decreased by nearly an order of magnitude, as compared to the known state-of-the-art.

### ACKNOWLEDGMENTS

This work was supported by the US National Science Foundation under Award Number #1722127, SBIR Phase I: Integrated Thermoelectric Heat Exchanger (iTEG-HX) for Carbon Neutral Electricity Production through Recovery of Cold Energy from Regasification of LNG.

### REFERENCES

1. A.F. Ioffe, *Semiconductor Thermoelements and Thermoelectric Cooling* (London: Infosearch, 1957).
2. Y.M. Lobunets, *Thermoelectricity* 2, 65 (2014).
3. S. Carnot, *Reflections on the Motive Power of Heat* (New York: John Wiley & Sons, 1890).
4. J.P. Heremans, M.S. Dresselhaus, L.E. Bell, and D.T. Morelli, *Nat. Nanotechnol.* 8, 471 (2013).
5. Y.M. Lobunets, Patent UA125129 (2018).
6. T.C. Harman, J.H. Cahn, and M.J. Logan, *Appl. Phys.* 30, 1351 (1959).
7. S. LeBlanc, S.K. Yee, M.L. Scullin, C. Dames, and K.E. Goodson, *Renew. Sustain. Energy Rev.* 32, 313 (2014).
8. T.J. Hendricks, S. Yee, and S. LeBlanc, *J. Electron. Mater.* 45, 1751 (2016).
9. S.K. Yee, S. LeBlanc, K.E. Goodson, and C. Dames, *Energy Environ. Sci.* 6, 2561 (2013).
10. Cryogenic power generation system recovering LNG's cryogenic energy and generating power for energy and CO<sub>2</sub> emission savings. [http://www.osakagas.co.jp/en/rd/technical/1198907\\_6995.html](http://www.osakagas.co.jp/en/rd/technical/1198907_6995.html).
11. W. Sun, P. Hu, Z. Chen, and L. Jia, *Energy Convers. Manag.* 46, 789 (2005).
12. M. Kambe, R. Morita, K. Omoto, Y. Koji, T. Yoshida, and K. Noishiki, *Power Energy Syst.* 2, 1304 (2008).